JOURNAL OF ENVIRONMENTAL SCIENCES 117 (2022) 295–304

Available online at www.sciencedirect.com

ScienceDirect

www.elsevier.com/locate/jes

JES JOURNAL OF ENVIRONMENTAL SCIENCES

www.jesc.ac.cn

Evaluation of disinfection byproducts for their ability to affect mitochondrial function

George William Kajjumba[1], *Rachael E. Bokota*[2], *Matias Attene-Ramos*[2], *Erica J. Marti*[1,*]

[1] *Department of Civil and Environmental Engineering, University of Nevada, Las Vegas, NV, USA*
[2] *Department of Environmental and Occupational Health, Milken Institute School of Public Health, George Washington University, Washington DC, USA*

ARTICLE INFO

Article history:
Received 15 March 2022
Revised 3 May 2022
Accepted 6 May 2022
Available online 21 May 2022

Keywords:
Disinfection byproducts
Toxicity
Mitochondrial membrane potential
Dose-response curve
In vitro bioassay
Emerging contaminants

ABSTRACT

In the race to deliver clean water to communities through potable water reuse, disinfection and water quality assessment are and will continue to be fundamental factors. There are over 700 disinfection byproducts (DBPs) in water; evaluating each compound is practically impossible and very time consuming. A bioanalytical approach could be an answer to this challenge. In this work, the response of four major classes of DBPs toward mitochondrial membrane potential ($\Delta\Psi m$) and cytoplasmic adenosine triphosphate (C-ATP) was investigated with human carcinoma (HepG2) cells. Within 90 min of cell exposure, only the haloacetic acid (HAA) mixture caused a cytotoxic response as measured by C-ATP. All four groups (haloacetonitriles (HANs), trihalomethanes (THMs), nitrosamines (NOAs), and HAAs) responded well to $\Delta\Psi m$, $R^2 > 0.70$. Based on the half-maximum concentration that evoked a 50% response in $\Delta\Psi m$, the response gradient was HANs >> HAAs ~ THM > NOAs. The inhibition of the $\Delta\Psi m$ by HANs is driven by dibromoacetonitrile (DBAN), while dichloroacetonitrile (DCAN) did not cause a significant change in the $\Delta\Psi m$ at less than 2000 μM. A mixture of HANs exhibited an antagonistic behavior on the $\Delta\Psi m$ compared to individual compounds. If water samples are concentrated to increase HAN concentrations, especially DBAN, then $\Delta\Psi m$ could be used as a biomonitoring tool for DBP toxicity.

Introduction

Water is a cardinal pillar of life; to remove microbes, dissolved salts, and other contaminants, technologies like membrane-filtration, coagulation, adsorption, ultraviolet (UV) irradiation, ozone, chloramination, and chlorination are used (Jiang et al., 2016; Keucken et al., 2017; Sharma et al., 2019; Watson et al., 2012). Physical methods (e.g., coagulation and adsorption) incompletely remove organic matter and pathogens; thus, the use of chlorination, ozone, and UV is needed for disinfection. The implementation of chemical disinfectants leads to toxic disinfection byproducts (DBPs). Over 700 DBPs have been discovered in water (Richardson, 2011), including halogenated and nonhalogenated, carbonaceous and nitrogenous, and organic and inorganic compounds. The major classes of DBPs include trihalomethanes (THMs), haloacetic acids (HAAs), haloacetonitriles (HANs), halonitromethanes (HNMs), haloacetamides (HAMs), and nitrosamines (NOAs) (Pressman et al., 2010; Weinberg et al., 2002). Brominated and iodinated DBPs top the toxicity list of DBPs (Cortés and Marcos, 2018). DBP formation and concentrations are driven by the disinfection method and the quantity of organic matter in water

* Corresponding author.
E-mail: erica.marti@unlv.edu (E.J. Marti).

https://doi.org/10.1016/j.jes.2022.05.014
1001-0742/

(Li and Mitch, 2018), which demonstrate the dependence of water quality on treatment technologies.

Although the adverse effects of many DBPs are not fully known, DBPs are reported to be cytotoxic, carcinogenic, and/or genotoxic to several species. Epidemiological studies have found links between DBP exposure and bladder/colon cancer, abortion, and low birth weight (Costet et al., 2011; Gallagher et al., 1998; Villanueva-Ponce et al., 2015). THMs are mutagenic to *Salmonella typhimurium* TA1535 strain (Pegram et al., 1997), and their toxicity is mediated by the induction of glutathione S-transferase metabolic activity (Schlosser et al., 2015). THMs affect mitochondria performance through Rhodamine 123 inhibition (Hartig et al., 2005). Nitrosamines are linked to producing thiobarbituric acid reactive substances in rats (Hassan and Yousef, 2010). Also, *N*-nitrosodimethylamine (NDMA), the most frequently detected compound in the NOA class, induces Noxa and puma proteins in the apoptosis of mitochondria in mammalian cells (Iwaniuk et al., 2019). HAAs inhibit glyceraldehyde-3-phosphate dehydrogenase, reducing cytoplasmic adenosine triphosphate (ATP) (Dad et al., 2018). Dichloroacetonitrile (DCAN) forms histopathological alterations, generating hepatic sinus dilation, hemorrhage, vacuolar degeneration, and renal tubular swelling (Dong et al., 2018). The acute toxicity of HANs is related to cyanide ion release. Cyanide attenuates mitochondrial function by decreasing succinate dehydrogenase, citrate synthase, and complex I, IV, and V performance (Zhang et al., 2021). Though DBPs may have common precursors and result from a common disinfection process, their toxicity mechanisms and endpoints vary for different DBP classes.

To detect and quantify DBPs, machines like mass spectrometry (MS) have been widely employed. However, the intense capital investment in MS precludes most low-income communities from monitoring DBPs. In addition, the time involved in MS sample preparation makes it hard to detect DBPs in real time; thus, using MS to detect DBPs can be equated to postmortem analysis. Cell bioassays are a promising approach to detecting and quantifying water quality; they can be cheap and reliable in detecting contaminants (US EPA, 2018). When cells are exposed to contaminants, a quantifiable change in endpoint like proliferation, cytotoxicity, metabolic activity, viability, mitochondrial membrane potential ($\Delta\Psi m$), among others, can be observed (Baderna et al., 2019).

Chemicals enter the cell either by passive or active transport. The latter is energy intense; it can quickly plummet cytoplasmic ATP (C-ATP) and affect the mitochondrial membrane potential, $\Delta\Psi m$ (Nicholls and Budd, 2000). The state of $\Delta\Psi m$ is an important index of the bioenergetic state of a cell. Live or fast-growing cells exhibit higher $\Delta\Psi m$ than senescent cells (Dong et al., 2018; Huang, 2002). The changes in $\Delta\Psi m$ can be noticed in less than two hours upon cell exposure to a contaminant (Sakamuru et al., 2016).

Given the quick response of $\Delta\Psi m$ and C-ATP to energy-consuming pollutants, some studies have applied them to investigate the toxicity of DBPs. Chen and team investigated the response of mitochondria in the presence of chloroacetic acid (CAA) and found that CAA attenuates mitochondria performance through $\Delta\Psi m$ loss (Chen et al., 2013). However, the study was limited to only CAA. In another study, DBPs induced toxicity by reducing ATP carrier SLC25A6 genes (Chen et al., 2019). This study was limited to only three compounds from three different classes of DBPs. Dad et al. (2018) studied the cytoplasmic ATP during HAA exposure. They found that HAAs inhibit cell function by affecting pyruvate dehydrogenase complex activity (Dad et al., 2018, 2013). Though mono-, di-, and tri-HAA were covered in this study, the behavior of major classes like NOAs and HANs is lacking. Other studies that have investigated the response of $\Delta\Psi m$ and ATP include Dong et al. (2018), Faustino-Rocha et al. (2016), and Hong et al. (2018). Though these studies have established the relationship between individual DBPs and mitochondria, there is a lack of information on how different DBP mixtures respond to $\Delta\Psi m$ and C-ATP. This study addresses the research gap by investigating mixtures of major classes of DBPs.

1. Methods and materials

1.1. Chemicals and reagents

The tested DBPs (see Section 1.4) were purchased from AccuStandard® (New Haven, CT, USA), Alfa Aesar (Ward Hill, MA, USA), and Beantown chemical (Hudson, NH, USA); the purity of the compounds was at least 98%. Fetal bovine serum (FBS) cell supplement and Eagle's minimum essential medium (EMEM) were obtained from ATCC™ (Manassas, VA, USA), while penicillin-streptomycin solution (PSS) and trypan blue were obtained from Hyclone™ (South Logan, UT, USA). Carbonyl cyanide-p-trifluoromethoxyphenylhydrazone (FCCP) was purchased from Sigma-Aldrich (St. Louis, MO, USA). The 200X signal enhancer, 10X buffer solution, and $\Delta\Psi m$ indicator were obtained from Codex™ (Gaithersburg, MD, USA). CellTiter-Glo® and CellTiter-Blue® were purchased from Promega (Madison, WI, USA).

1.2. Cell culture

The HepG2 cells were cultured based on the distributor's protocol and previously described elsewhere (Attene-Ramos et al., 2015; Kajjumba et al., 2021; Sakamuru et al., 2016). In summary, the deep-frozen preserved cells were thawed and cultured in a T-75 flask containing 89% EMEM, 10% FBS, and 1.0% PSS. The cells were incubated at 37.0 ± 0.5°C in a 5.0% ± 0.2% CO_2 environment. After attaining 60%–90% confluence, the cells were passed to a new flask and/or seeded in a 96 black-wall, clear-bottom plate (Greiner Bio-One North America, Monroe, NC) for subsequent experiments.

1.3. ΔΨm and C-ATP assays

The $\Delta\Psi m$ and C-ATP (cytotoxicity) assay protocols can be found in our previous study (Kajjumba et al., 2021). The plates were seeded with 50 µL of 800,000 cells/mL at 37.0°C in a 5.0% CO_2 environment. After 4.0 hr, the cell culture medium was removed and replaced with a medium containing different concentrations of DBPs; for HAAs, NOAs, and HANs, the volume was 50 µL. However, for volatile THMs (partial pressure > 5.0×10^{-4} atm/(m^3·mol)), the wells were filled with 350 µL to reduce headspace partitioning, and the plates were covered

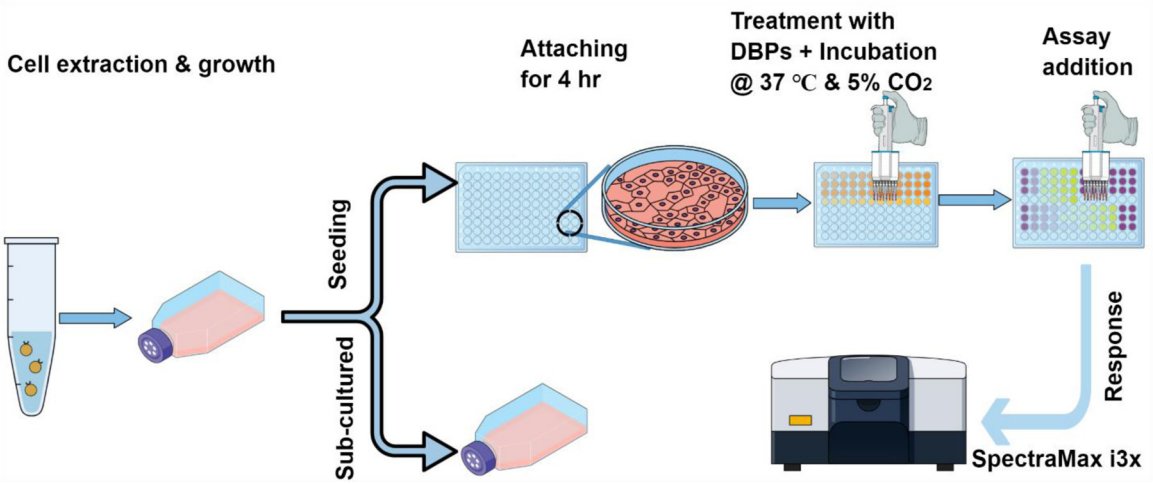

Fig. 1 – Assay preparation; each assay was modified based on this procedure.

with an alumina seal. It is important to note that the solubility level of the DBPs must not be exceeded in the solution. The solvent concentration in the cell culture medium (V/V) was kept below 1.0% to eliminate toxic effects from the solvents (e.g., methanol, acetone). The treatment stage was accomplished by incubating the plates for 60 min at 37.0 °C in a 5.0% CO_2 environment. After the treatment stage with DBPs, 50 µL of ΔΨm indicator were added to HAAs, NOAs, and HANs treated cells. For THMs, ~300 µL were removed, and to the remaining 50 µL of cell culture medium, 50 µL of ΔΨm indicator were added. After adding the ΔΨm indicator, the plates were incubated again for another 30 min before measuring the fluorescence on a SpectraMax i3x microplate reader; the steps are summarized in Fig. 1. For C-ATP measurement, either 50 µL of CellTiter-Glo® were added immediately after reading ΔΨm response or a separate set of experiments was conducted. As determined during method validation, the ΔΨm indicator does not interfere with the CellTiter-Glo® luminescence. The relative activity of ΔΨm or C-ATP amount was estimated using Eq. (1). Here, A_s is the fluorescence or luminescence (F/L) of a sample, B_{PC} is the F/L of the positive control—used to eliminate the effect of the background "noise," and C_{NC} is the F/L of the negative control. FCCP was used as a positive control, resulting in complete disruption of ΔΨm at 2000 µmol/L (Sakamuru et al., 2016). The cell culture medium was used as a negative control to represent no DBP treatment. For quality assurance and control, at least two separate experiments were conducted for each test in triplicate. In total, each data point represents at least three independent replicates. Data were analyzed using Origin 2020b software. Sigmoidal logarithmic dose-response curves were generated to estimate effective concentrations, $EC_{1.5}$ and EC_{50}.

$$\text{Relative } \Delta\Psi \text{ m or C} - \text{ATP} = \frac{A_s - B_{PC}}{C_{NC} - B_{PC}} \quad (1)$$

1.4. *DBP mixtures*

The HAN mixture was composed of four compounds, DCAN, DBAN, TCAN, and BCAN (HAN-4), while the HAA mixture was composed of five chemicals, namely CAA, DCAA, TCAA, BAA, and BCAA (HAA-5). The THM mixture was made from four compounds: BF, CF, DCBM, and DBCM (THM-4). The nitrosamine mixture was prepared from NDEA, NDMA, NDPhA, NDPA, NMEA, NMOR, NPIP, and NPYR (NOA-8). For each mixture, the individual chemical concentration (in molarity) was the same.

1.5. *Additivity, antagonistic and synergistic effects of DBPs*

Different models are proposed to estimate the additivity, antagonistic, and synergistic (AAS) effects of drugs, pharmaceuticals, pesticides, and contaminants. Rider and Simmons, in their book, meticulously described the different AAS models that have been developed since the 1920s (Rider et al., 2018). In this study, a Chou-Talalay model was used to estimate the AAS of HANs (Chou, 2010). Data for individual HANs were fitted to generate a fixed combination ratio to the median-effect equation, Eq. (2).

$$f_a = 1/[1 + (D_m/D)^m] \quad (2)$$

Here, f_a represents the fraction of affected ΔΨm, D_m is the median-effect dose, D is the dose, and m is the slope. The Chou-Talalay model combines the Hill, Henderson-Hasselbalch, Michaelis-Menten, and Scatchard equations to develop a robust model that can predict the combined effect of drugs/contaminants. The model relies on the combination index (CI). When the CI > 1.0, the compounds are antagonistic. If the CI < 1.0, the compounds are synergistic, and CI =1 indicates additive effects (Rider et al., 2018). The CI is calculated first by fitting data from each contaminant alone, and a fixed ratio combination of a contaminant to the median effect is established. The rearranged Hill and Michaelis-Menten equations establish the unknown dose effect. The CI value is then calculated from the resulting parameter estimates using Henderson-Hasselbalch and Scatchard equations. CompuSyn software (Paramus, NJ, USA) was used to calculate the CI, and the step-by-step application of the model can be found on the developers' YouTube channel (Chou, 2017).

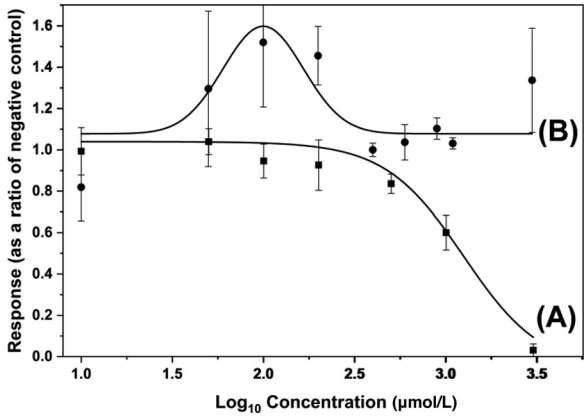

Fig. 2 – (A) ΔΨm and (B) C-ATP response at different THM-4 concentrations. Treatment time = 90 min, cells per well = 40,000, cell culture medium volume per well = 350 μL. Each data point represents a mean of 3-8 independent values, and error bars show one standard deviation.

2. Results and discussion

2.1. *Trihalomethanes*

The four compounds in THM-4 were chosen because of their relatively high abundance in treated water. The effect of THM-4 on ΔΨm and C-ATP was tested at 10, 50, 100, 200, 500, 1000, and 3000 μmol/L; at each concentration, the amount of each individual compound was equal (i.e., the 10 μmol/L test contained 2.5 μmol/L of each THM). Following ΔΨm and C-ATP measurement, the number of viable cells was calculated with CellTiter-Blue®. The negative control (untreated cells) elicited a response of 114.0% ± 11.1%, while the positive control (FCCP treated cell) induced a response of 0.0 ± 0.1%.

Fig. 2A shows the response of HepG2 ΔΨm at varying THM-4 concentrations; no significant drop in ΔΨm was observed at less than 500 μmol/L. HepG2 cells put up a strong resistance towards THM toxicity. The THM-4 mix that caused a 1.5% decrease ($EC_{1.5}$) in ΔΨm compared to the untreated control was 877.6 μmol/L. However, as the concentration increased, the ΔΨm plummeted at 1000 μmol/L. The half-maximum THM-4 mix concentration that evoked a 50% decrease (EC_{50}) in the ΔΨm was 1024.0 μmol/L. At 2000 μmol/L, the ΔΨm was totally lost, giving a response of 0.0 ± 3.7%. To ascertain that the drop in ΔΨm was not from apoptosis, a parallel cell viability response was conducted using the CellTiter-Blue® protocol. At 3000 μmol/L, the response of viable cells compared to negative control was 103.2% ± 2.1%. Thus, the decrease in ΔΨm is attributed to the disruption of the ΔΨm only. C-ATP was measured using the CellTiter-Glo® protocol. Fig. 2B shows the change in C-ATP; a maximum gain in ATP response is observed at 100 μmol/L (152.10% ± 31.25%), and C-ATP did not drop below that of the negative control. Using the luminescent-based Microtox assay (*Aliivibrio fischeri* strains), individual chlorinated and brominated THMs were observed to trigger EC_{50} at 10^{-4} to 10^{-2} mol/L (Stalter et al., 2016). The THM mixture in this study elicited a similar response towards ΔΨm, $EC_{50} = \sim 10^{-3}$ mol/L.

Several toxicity studies have considered the toxicity of individual THMs rather than the whole THM family (Hartig et al., 2005; Komaki and Ibuki, 2022; Stalter et al., 2016). At the individual level, the toxic potency of THMs is reported to be driven by iodinated THMs, followed by brominated THMs, and then chlorinated THMs (Stalter et al., 2016). Previous studies have linked the loss of ΔΨm to glucose uptake, acceleration of lactate production, and mitochondrial permeability transition damage (Burke et al., 2007; Hartig et al., 2005). Chloroform facilitates the biotransformation of cytochrome P450 that leads to phosgene formation, a reactive oxygen species (ROS) that can efficiently react with ΔΨm proteins (de Castro Medeiros et al., 2019; Hartig et al., 2005). When rats were administered with different THM compounds, THMs lowered the activity of succinate dehydrogenase and ATP synthase (Faustino-Rocha et al., 2016). This interferes with the electron transport chain, which in return affects ATP synthesis. However, in our study, the measurement of cytoplasmic ATP with CellTiter-Glo® elicited a different observation—cytoplasmic ATP remained relatively the same. When cells are exposed to THMs, ROS are generated. Through an orchestrated mechanism, ROS scavengers (e.g., catalase) are accumulated to prevent the cell from further damage (de Castro Medeiros et al., 2019). The accretion of glutathione and the triggering of the ROS defense mechanism increases respiratory activity and cell bioenergy.

2.2. *Haloacetic acids*

HAAs are among the regulated DBPs in the drinking water industry. They are formed mainly as a result of disinfecting water with chlorine. They have a low vapor pressure, less than 5.0×10^{-7} atm/(m^3·mol), and they can easily absorb into the bloodstream after ingestion (Parvez et al., 2019). And because of this low vapor pressure, they do not vaporize at bathing water temperatures, making it easier to penetrate the skin (Cardador and Gallego, 2011). The US Environmental Protection Agency (EPA) regulates BAA, CAA, DCAA, DBAA, and TCAA at a maximum level of 60 μg/L (Pals et al., 2011; US EPA, 2006). We studied the effect of a mix of CAA, DCAA, TCAA, BAA and BCAA (HAA-5) on ΔΨm and C-ATP. After allowing cells to attach to the well plate, each well was treated with 50 μL of the respective HAA-5 concentration (10–3000 μmol/L). Because of the low partial pressure, headspace within the well was considered acceptable. During the ΔΨm assessment, negative and positive controls averaged at 111.7% ± 3.3% and 0.0 ± 0.1%, respectively. For C-ATP, the negative control was 100% ± 10.9%, and the positive control was 0.0 ± 0.2%. HAA-5 did not show a severe effect on ΔΨm; at 500 μmol/L, the reduction in ΔΨm compared to the negative control was 89.1% ± 8.3%. The HAA-5 concentration that caused an EC_{50} effect was 995.5 μmol/L, Fig. 3A. However, the reduction in ΔΨm could also be attributed to HAAs' cell cytotoxicity. At 1000 μmol/L, HAA-5 attenuated viable cells to 53.9% ± 1.8%, Fig. 3B.

When the ΔΨm response dropped to half (EC_{50} = 995.5 μmol/L), the cytoplasmic ATP plummeted to 53.9% ± 1.8%. Glyceraldehyde 3-phosphate dehydrogenase (GAPDH) plays a central role in glycolysis. Mono-HAAs

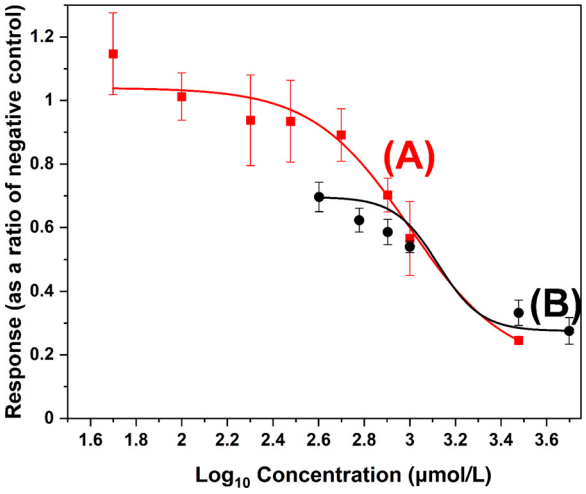

Fig. 3 – (A) ΔΨm and (B) C-ATP response at different HAA-5 concentrations. Treatment time = 90 min, cells per well = 40,000, cell culture medium volume per well = 50 μL. Each data point represents a mean of at least four independent values, and error bars show one standard deviation.

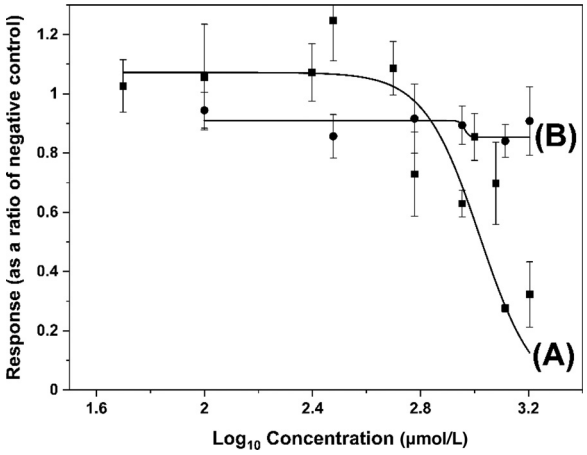

Fig. 4 – ΔΨm (A) and (B) C-ATP response at different NOA-8 concentrations. Treatment time = 90 min, cells per well = 40,000, volume of medium per well = 50 μL. Each data point represents a mean of at least four independent values, and error bars show one standard deviation.

have been linked to GAPDH blockage, which inhibits the formation of pyruvate that is needed for mitochondria metabolism (Pals et al., 2013). Di-HAAs, especially DCAA, have been reported to increase cytoplasmic ATP (Dad et al., 2018); however, they do not inhibit cytoplasmic ATP through GAPDH introversion. In the presence of magnesium ions, the pyruvate dehydrogenase complex (PDC) enzyme increases the conversion of pyruvate to acetyl-CoA (De Marcucci and Lindsay, 1985). When a cell is exposed to di- or tri-HAAs, PDC enzyme activity increases, inhibiting pyruvate dehydrogenase kinase, further increasing ATP production (Dad et al., 2018; De Marcucci and Lindsay, 1985; Frey et al., 1989). In this study, the overall ATP production decreased when the cells were exposed to a mixture of HAAs composed of mono-, di-, and tri-HAAs. This suggests that the inhibition of ATP in a cell exposed to an HAA mixture will be through GAPDH obstruction. We hypothesize that in drinking water, the overall toxicity of HAAs will be driven by mono-HAAs like CAA and BAA, which fits with toxicity results for multiple endpoints as reported by Stalter et al. (2016) and Muellner et al. (2007). Thus, during water quality assessment, monitoring CAA and/or BAA in water samples can provide a good benchmark for the toxicity contributed by HAAs.

2.3. *Nitrosamines*

In water treatment, NOAs are a result of ozonation and chloramination disinfection (Gerrity et al., 2015; Marti et al., 2015). Among the NOAs, NDMA is detected the most in drinking water; it is regulated at 10.0 ng/L in Australia and at 40 ng/L in Canada (Gerrity et al., 2015; Minister of Health of Canada, 2011). Eight NOAs (NDEA, NDMA, NDPhA, NDPA, NMEA, NMOR, NPIP, and NPYR) were mixed at equal molar concentrations (50-1600 μmol/L). After allowing cells to attach to the well plate, 50 μL of respective NOA-8 mix at concentrations 50-1600 μmol/L were added to the cells. Because of the low partial pressure (less than 7.0×10^{-6} atm/(m^3·mol)), headspace within the well was considered acceptable. After incubating the cells with NOA-8, ΔΨm and cell cytotoxicity were measured. The negative and positive control for ΔΨm were 112.6% ± 19.9% and -2.6% ± 7.5%, respectively. For C-ATP, the relative activity for the negative control was 105.6% ± 1.4% and the positive control was 0.0 ± 0.3%. The NOA-8 mix did not elicit cytotoxic effects; the ATP remained relatively constant throughout the tested range, Fig. 4B. At 1600 μmol/L, the C-ATP ratio compared to the unexposed cells was 90.8% ± 11.6%. However, at elevated concentrations, NOA-8 affected the ΔΨm, Fig. 4A. The $EC_{1.5}$ for NOA-8 was 244.1 μmol/L, while the half-maximum concentration that caused a 50% reduction in ΔΨm was 1468 μmol/L. Compared to HAA-5 and THM-4 mixtures, NOA-8 elicited the least effect on ΔΨm.

The ability of NOAs to affect mitochondrial bioenergetics has been employed as a model to study the effect of oxidative stress, metabolism, phosphorylation, and cachexia injury in muscles (Antunes et al., 2014; Oliveira et al., 2013; Yang et al., 1990). Mitochondria play a crucial role in energy production and cell death. They control apoptosis by regulating proteins such as Bax, Bad, Bcl-2, Bcl-xL, and glutathione peroxidase; these proteins control the ΔΨm. In excess of Bcl-2 and/or Bcl-xL, the ΔΨm is lost, facilitating the opening of mitochondrial pores, which revokes the release of apoptosis-inducing proteins like cytochrome C (Laothong et al., 2013). This further disrupts the electron transport between Complex I and IV (Dinamarco et al., 2010). Cell exposure to NOAs attenuates antioxidant proteins, glutathione peroxidase, and phosphatidylglycerol that controls the lipid-ion channels of the membrane (Antunes et al., 2014; Laothong et al., 2013). The attenuation of phosphatidylglycerol suggests the loss of ΔΨm. However, NOA-8 did not show signs of cytotoxicity since the levels of C-ATP remained relatively constant. Thus, we hypothesize that NOAs do not cause the excessive escape of cytochrome C. This

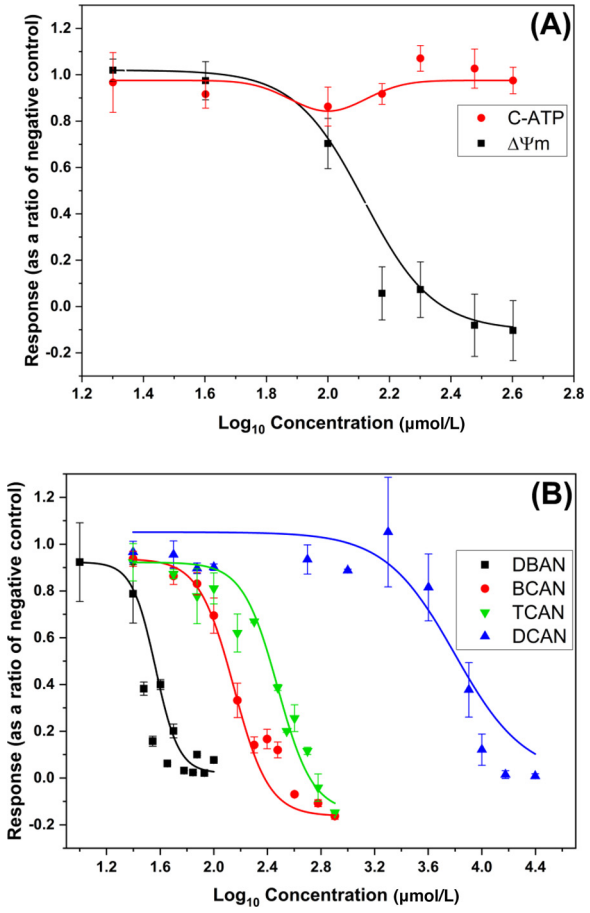

Fig. 5 – Dose-response curves of (A) HAN-4 on C-ATP and ΔΨm (B) DBAN, BCAN, TCAN, and DCAN effect on ΔΨm. Treatment time = 90 min, cells per well = 40,000, and volume of medium per well = 50 μL. Each data point represents a mean of 5-8 independent values, and error bars show one standard deviation.

might explain why the effect of NOA-8 was less compared to HAA-5 and THM-4 mixtures.

2.4. *Haloacetonitriles*

HANs are an emerging and unregulated class of DBPs that are formed in water as a result of chlorination and chloramination. There are different forms of HANs in water; the most common include BCAN, DBAN, DCAN, and TCAN (Lipscomb et al., 2008). When we measured HAN concentrations in drinking water, they ranged from non-detectable levels (<0.1 μg/L) to 5.5 μg/L (Unpublished results), with DCAN topping the list. This is in agreement with other studies where DCAN and other dihalogenated HANs are the most frequently detected (Bond et al., 2015; Krasner et al., 1989; Liew et al., 2016). A mixture of four HANs (HAN-4; BCAN, DBAN, DCAN, TCAN) was used in this study. Fig. 5A elicits no effect of HAN-4 on C-ATP; however, the HAN-4 mix negatively affected ΔΨm. At 130.5 μmol/L, HAN-4 induced a 50% reduction in the ΔΨm activity, while at 40.6 μmol/L, a noticeable change in ΔΨm was observed ($EC_{1.5}$). Among DBP classes, the HAN class had a potent effect on ΔΨm. Based on the EC_{50} for the ΔΨm assay, the toxicity trend for DBP mixtures is HAN-4 >> HAA-5 ~ THM-4 > NOA-8 (Table 1).

Table 1 – Effective concentrations of DBPs on the ΔΨm.

	$EC_{1.5}$ (μmol/L)	EC_{50} (μmol/L)	R^2 [a]
HAA-5	129.0	995.5	0.993
NOA-8	244.1	1468.0	0.715
THM-4	877.6	1024.0	0.965
HAN-4	40.62	130.5	0.998
DBAN	15.30	28.84	0.863
BCAN	24.95	147.5	0.975
DCAN	2607.0	7054.0	0.980
TCAN	31.02	415.8	0.974

R^2 is the coefficient of determination for the regression analysis upon which the EC values were calculated. [a] Data is significant at $\rho < 0.05$.

Due to the potent effect elicited by the HAN-4 mix on ΔΨm, the effect of individual HANs was expounded to compare the change in ΔΨm. The relative ΔΨm responses of cells after 90 min of DBAN, BCAN, TCAN, and DCAN exposure are shown in Fig. 5B. The ΔΨm decreased as the number of bromide ions and chloride ions in a given compound increased. The potency gradient of HANs was DBAN >> BCAN > TCAN >>> DCAN. DCAN hardly affected the ΔΨm; at 4000 μmol/L, the ΔΨm was 81.5% ± 14.3%. To achieve a 50% reduction in ΔΨm with DCAN, a concentration of 7054 μmol/L is needed. This level is over 54 times the EC_{50} value of the HAN-4 mix (130.5 μmol/L). The potency of TCAN and BCAN on ΔΨm was moderate compared to the HAN-4; EC_{50} values were 415.8 and 147.5 μmol/L, respectively, for TCAN and BCAN. DBAN elicited the strongest effect on the ΔΨm of HepG2 cells. An increase in DBAN concentration from 10 to 60 μmol/L plummeted the ΔΨm activity from 92.3% ± 16.8% to 3.2% ± 0.1%. At 28.84 μmol/L, DBAN reduced the ΔΨm by 50% compared to the untreated cells. These results reveal that DBAN drives the potency of HAN-4. If used as a biomonitoring tool, the ΔΨm assay could be used to detect DBAN at concentrations ≥ 30 μmol/L (6 mg/L); however, this is orders of magnitude above reported concentrations in drinking water. Consequently, samples would require extraction and concentration prior to using this bioassay.

The acute toxicity of HANs can be attributed to their metabolism by the cell to a potentially toxic compound-cyanide, CN^- (Lipscomb et al., 2008). The presence of CN^- and other related metabolites (acylating agent and reactive ketone) can bind and inhibit thiol-containing proteins responsible for cellular respiration (Pals et al., 2016). Impeding the oxidative phosphorylation respiratory chain could generate ROS responsible for the ΔΨm decrease. When rats were administered 750 (μmol/L)/kg HAN, thiocyanate excretion followed a trend of BCAN > DCAN > DBAN > TCAN (Lin et al., 1986). In our study, the weakening of ΔΨm is in the order of DBAN >> BCAN > TCAN >>> DCAN. The number of bromine atoms in a compound dictated the declining ΔΨm, followed by the number of chlorine atoms. This observation can be explained by the nucleophilic substitution (S_{N2}) tendency of halogens. The cyano group in HANs is attached to an α-carbon with halogen sub-

stitution through S_{N2}. Both the cyano group and the α-carbon act as reactive centers. The S_{N2} potency of an alkyl bromide [$\sim 7 \times 10^{-3}$ mol/L] is 8.5 times higher than that of an alkyl chloride [$\sim 6 \times 10^{-2}$ mol/L] (Schwarzenbach et al., 2003). Bromine has a stronger leaving tendency than chlorine (Lu et al., 2018). Thus, bromide compounds will make the cyano carbon more electrophilic, rendering it a more reactive compound compared to chlorinated HANs.

2.5. *Additivity, antagonistic and synergistic (AAS) of HANs*

Contaminants in the water system can exist as single compounds or as groups; the latter applies to DBPs in water quality assessment. Most studies look at individual compounds, but it is not clear if a mixture should be estimated as the sum of individual toxicities or if the toxicity of multiple compounds is greater or lower due to synergistic or antagonistic effects. Therefore, we compared mixtures and individual compounds for their impact on $\Delta\Psi m$. Among the tested DBP mixtures, HANs gave a strong response to $\Delta\Psi m$; thus, HANs were selected for this investigation. The individual HANs (DBAN, BCAN, TCAN, and DCAN) were mixed at a molar ratio of 1:1:1:1 to make HAN-4 concentrations of 100, 200, 300, and 400 µmol/L. Fig. 6A elicits the CI plot of HAN-4, and Fig. 6B shows individual toxicity at the tested concentrations. DCAN and TCAN contributed the least toxicity to the $\Delta\Psi m$ damage, while DBAN drove most of the toxicity. HANs elicited an antagonistic behavior at all tested concentrations. At a higher concentration (300 and 400 µmol/L), both DBAN and BCAN can plummet $\Delta\Psi m$ to zero with no room left for TCAN and DCAN to induce toxicity. However, the cause of antagonistic behavior at lower concentrations is not well known. More data are needed for statistical confirmation of the trend. Studies should be conducted with varying low concentrations (25-100 µmol/L) of HANs to complement this study where all HANs were equal concentration. If HANs are antagonistic at lower concentrations, it could limit the applicability of the $\Delta\Psi m$ assay since it reduces the sensitivity of the assay at low concentrations.

2.6. *Solvent effect on $\Delta\Psi m$*

In most drinking waters, DBPs exist at ng/L and µg/L levels; direct measurement, either through analytical or bioanalytical techniques, requires concentrating samples through extraction. DBPs are concentrated from water into solvents like methyl tert-butyl ether (MTBE), methanol, dimethyl sulfoxide (DMSO), dichloromethane, and acetone, among others. In addition, analytical standards are sold in such solvents. The question is, how much solvent concentration can interfere with the bioassay measurements? Fig. 7 elicits the changes in the $\Delta\Psi m$ at varying volume ratios (V/V) for DMSO, MTBE, and methanol. $\Delta\Psi m$ was not affected by methanol up to 5%, whereas an effect was seen with 1.5% DMSO. MTBE and dichloromethane had the strongest effect on $\Delta\Psi m$. At 5.0%, MTBE was responsible for 97.2% ± 1.5% $\Delta\Psi m$ loss. Dichloromethane is not included in Fig. 7 because even the lowest amount (0.25%) resulted in total $\Delta\Psi m$ loss, and the solvent deteriorated the plastic well plate. Thus, extreme care must be taken in experiments where DBPs are dissolved in MTBE and dichloromethane; otherwise, the response seen could be driven by these solvents and not DBPs themselves. Although sample extraction into a solvent raises the concentration of DBPs, it would be necessary to then dilute the extract prior to use in a bioassay to avoid solvent effects. In pursuit of finding a bioanalytical tool for monitoring drinking water quality, there is a need to find better ways of extracting DBPs into a solvent suitable for bioassay work.

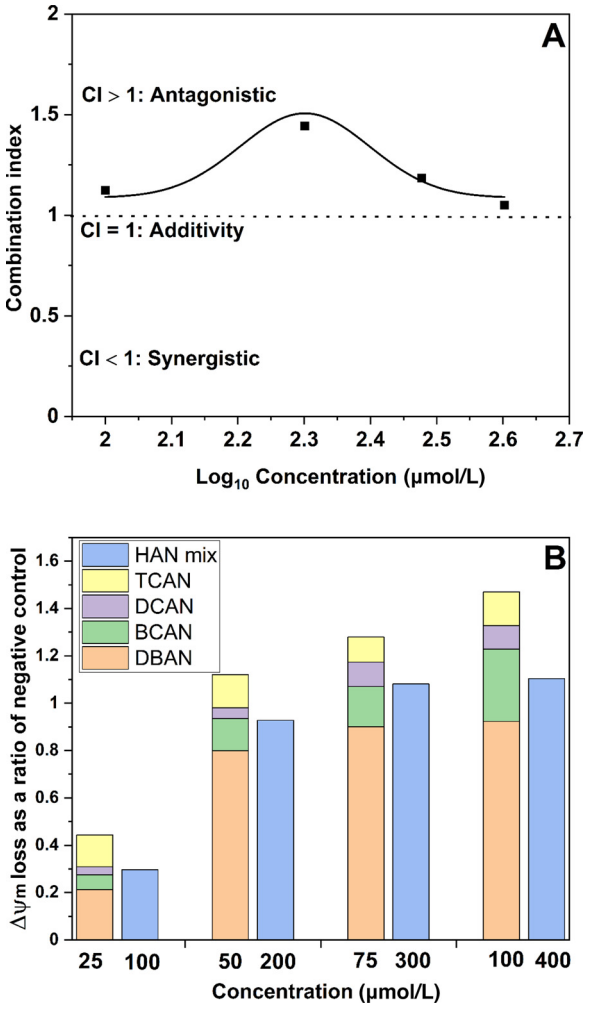

Fig. 6 – (A) Additivity, antagonistic and synergistic (AAS) response based on Chou-Talalay model, (B) experimental data at 100, 200, 300, 400 µmol/L HAN-4; the mixture molar ratio is 1:1:1:1 for individual compounds. Individual $\Delta\Psi m$ effect was conducted at 25, 50, 75, and 100 µmol/L. The AAS was modeled using the CompuSyn software (Paramus, NJ, USA) (Chou, 2010).

3. Conclusion

As water reuse is becoming a viable option to combat water scarcity, there is an increased risk of forming emerging DBPs. Measuring all known DBPs is time and cost prohibitive; therefore, there is a need to advance tools for measuring the over-

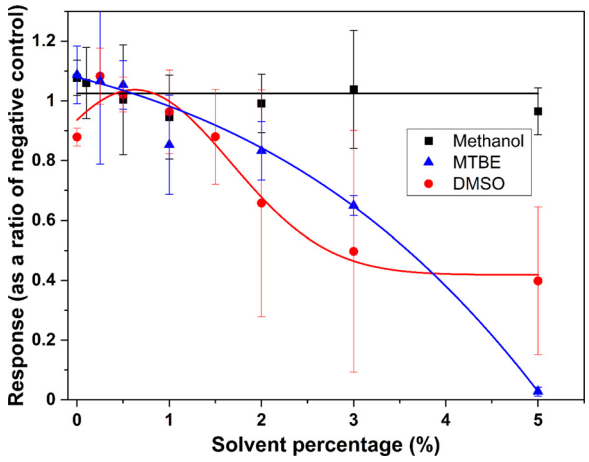

Fig. 7 – Effect of solvent (V/V) on ΔΨm. Exposure time = 90, cells per well = 40,000 cell, and volume of medium per well = 50 µL.

all toxicity of disinfected water rather than individual chemicals. The present work lays a foundation for assessing the DBP toxicity of concentrated samples with a fast *in vitro* bioassay. In summary, we were able to establish the short-term effects of the four major DBP classes on ΔΨm and C-ATP. The four groups of DBP mixtures tested were THM-4, HAA-5, NOA-8, and HAN-4. Targeting C-ATP as a quick bioanalytical assay did not yield a noticeable response in most DBP classes; only HAA was able to give a positive response. All compounds elicited a good correlation with ΔΨm. The half-maximum concentration that induced a 50% reduction in ΔΨm for NOA-8, THM-4, HAA-5, and HAN-4 was 1468.0, 1024.0, 995.5, and 130.5 µmol/L, respectively. The strong potency of HANs is based on their ability to form CN^-. Individual HANs decreased ΔΨm in the following order: DBAN >> BCAN > TCAN >>> DCAN. Bromine is a better leaving group compared to chlorine; therefore, brominated HANs are more electrophilic than chlorinated HANs. The number of bromine atoms in a compound dictates the disruption of ΔΨm, followed by the number of chlorine atoms. In pursuit of developing a cheap and reliable biomonitoring DBP tool, only HANs gave a strong response with the ΔΨm assay. For those conducting bioassay work, it is important to note that the use of solvents like MTBE and dichloromethane have a potent effect on ΔΨm, and the amount of solvent should be minimized as much as possible.

Acknowledgment

This material is based upon work supported by the National Science Foundation (No. 1833108).

REFERENCE

Antunes, D., Padrão, A.I., Maciel, E., Santinha, D., Oliveira, P., Vitorino, R., et al., 2014. Molecular insights into mitochondrial dysfunction in cancer-related muscle wasting. Biochim. Biophys. Acta 1841, 896–905. doi:10.1016/j.bbalip.2014.03.004.

Attene-Ramos, M.S., Huang, R., Michael, S., Witt, K.L., Richard, A., Tice, R.R., et al., 2015. Profiling of the Tox21 chemical collection for mitochondrial function to identify compounds that acutely decrease mitochondrial membrane potential. Environ. Health Perspect. 123, 49–56. doi:10.1289/ehp.1408642.

Baderna, D., Caloni, F., Benfenati, E., 2019. Investigating landfill leachate toxicity in vitro: A review of cell models and endpoints. Environ. Int. 122, 21–30. doi:10.1016/j.envint.2018.11.024.

Bond, T., Templeton, M.R., Mokhtar Kamal, N.H., Graham, N., Kanda, R., 2015. Nitrogenous disinfection byproducts in English drinking water supply systems: occurrence, bromine substitution and correlation analysis. Water Res. 85, 85–94. doi:10.1016/j.watres.2015.08.015.

Burke, A.S., Redeker, K., Kurten, R.C., James, L.P., Hinson, J.A., 2007. Mechanisms of chloroform-induced hepatotoxicity: oxidative stress and mitochondrial permeability transition in freshly isolated mouse hepatocytes. J. Toxicol. Environ. Health 70, 1936–1945. doi:10.1080/15287390701551399.

Cardador, M.J., Gallego, M., 2011. Haloacetic acids in swimming pools: swimmer and worker exposure. Environ. Sci. Technol. 45, 5783–5790. doi:10.1021/es103959d.

Chen, C.H., Chen, S.J., Su, C.C., Yen, C.C., Tseng, T.J., Jinn, T.R., et al., 2013. Chloroacetic acid induced neuronal cells death through oxidative stress-mediated p38-MAPK activation pathway regulated mitochondria-dependent apoptotic signals. Toxicology 303, 72–82. doi:10.1016/j.tox.2012.10.008.

Chen, Y., Xu, T., Yang, X., Chu, W., Hu, S., Yin, D., 2019. The toxic potentials and focus of disinfection byproducts based on the human embryonic kidney (HEK293) cell model. Sci. Total Environ. 664, 948–957. doi:10.1016/j.scitotenv.2019.01.361.

Chou, T., 2017. CompuSyn Video Ting Chao Chou [WWW Document]. YouTube URL.

Chou, T.C., 2010. Drug combination studies and their synergy quantification using the chou-talalay method. Cancer Res. 70, 440–446. doi:10.1158/0008-5472.CAN-09-1947.

Cortés, C., Marcos, R., 2018. Genotoxicity of disinfection byproducts and disinfected waters: A review of recent literature. Mutat. Res. Genet. Toxicol. Environ. Mutagen. 831, 1–12. doi:10.1016/j.mrgentox.2018.04.005.

Costet, N., Villanueva, C.M., Jaakkola, J.J.K., Kogevinas, M., Cantor, K.P., King, W.D., et al., 2011. Water disinfection by-products and bladder cancer: is there a European specificity? A pooled and meta-analysis of European case-control studies. Occup. Environ. Med. 68, 379–385. doi:10.1136/oem.2010.062703.

Dad, A., Jeong, C.H., Pals, J.A., Wagner, E.D., Plewa, M.J., 2013. Pyruvate remediation of cell stress and genotoxicity induced by haloacetic acid drinking water disinfection by-products. Environ. Mol. Mutagen. 54, 629–637. doi:10.1002/em.21795.

Dad, A., Jeong, C.H., Wagner, E.D., Plewa, M.J., 2018. Haloacetic acid water disinfection byproducts affect pyruvate dehydrogenase activity and disrupt cellular metabolism. Environ. Sci. Technol. 52, 1525–1532. doi:10.1021/acs.est.7b04290.

de Castro Medeiros, L., de Alencar, F.L.S., Navoni, J.A., de Araujo, A.L.C., do Amaral, V.S., 2019. Toxicological aspects of trihalomethanes: a systematic review. Environ. Sci. Pollut. Res. 26, 5316–5332. doi:10.1007/s11356-018-3949-z.

De Marcucci, O., Lindsay, J.G., 1985. Component X: An immunologically distinct polypeptide associated with mammalian pyruvate dehydrogenase multi-enzyme complex. Eur. J. Biochem. 149, 641–648. doi:10.1111/j.1432-1033.1985.tb08972.x.

Dinamarco, T.M., Figueiredo Pimentel, B.de C., Savoldi, M., Malavazi, I., Soriani, F.M., Uyemura, S.A., et al., 2010. The roles played by Aspergillus nidulans apoptosis-inducing factor

(AIF)-like mitochondrial oxidoreductase (AifA) and NADH-ubiquinone oxidoreductases (NdeA-B and NdiA) in farnesol resistance. Fungal Genet. Biol. 47, 1055–1069. doi:10.1016/j.fgb.2010.07.006.
Dong, Y., Li, F., Shen, H., Lu, R., Yin, S., Yang, Q., et al., 2018. Evaluation of the water disinfection by-product dichloroacetonitrile-induced biochemical, oxidative, histopathological, and mitochondrial functional alterations: Subacute oral toxicity in rats. Toxicol. Ind. Health 34, 158–168. doi:10.1177/0748233717744720.
Faustino-Rocha, A.I., Rodrigues, D., Gil da Costa, R.M., Diniz, C., Aragão, S., Talhada, D., et al., 2016. Trihalomethanes in liver pathology: Mitochondrial dysfunction and oxidative stress in the mouse. Environ. Toxicol. 31, 1009–1016. doi:10.1002/tox.22110.
Frey, P.A., Flournoy, D.S., Gruys, K., Yang, Y., 1989. Intermediates in reductive transacetylation catalyzed by pyruvate dehydrogenase complex. Ann. N. Y. Acad. Sci. 573, 21–35. doi:10.1111/j.1749-6632.1989.tb14984.x.
Gallagher, M.D., Nuckols, J.R., Stallones, L., Savitz, D.A., 1998. Exposure to trihalomethanes and adverse pregnancy outcomes. Epidemiology 9, 484–489. doi:10.1097/00001648-199809000-00003.
Gerrity, D., Pisarenko, A.N., Marti, E., Trenholm, R.A., Gerringer, F., Reungoat, J., et al., 2015. Nitrosamines in pilot-scale and full-scale wastewater treatment plants with ozonation. Water Res. 72, 251–261. doi:10.1016/j.watres.2014.06.025.
Hartig, S., Fries, S., Balcarcel, R.R., 2005. Reduced mitochondrial membrane potential and metabolism correspond to acute chloroform toxicity of in vitro hepatocytes. J. Appl. Toxicol. 25, 310–317. doi:10.1002/jat.1067.
Hassan, H.A., Yousef, M.I., 2010. Ameliorating effect of chicory (Cichorium intybus L.)-supplemented diet against nitrosamine precursors-induced liver injury and oxidative stress in male rats. Food Chem. Toxicol. 48, 2163–2169. doi:10.1016/J.FCT.2010.05.023.
Hong, H., Wu, H., Chen, J., Wu, B., Yu, H., Yan, B., et al., 2018. Cytotoxicity induced by iodinated haloacetamides via ROS accumulation and apoptosis in HepG-2 cells. Environ. Pollut. 242, 191–197. doi:10.1016/j.envpol.2018.06.090.
Huang, S.-G., 2002. Development of a high throughput screening assay for mitochondrial membrane potential in living cells. J. Biomol. Screen. 7, 383–389. doi:10.1177/108705710200700411.
Iwaniuk, A., Grubczak, K., Ratajczak-Wrona, W., Garley, M., Nowak, K., Jabłońska, E., 2019. N-nitrosodimethylamine (NDMA) induced apoptosis dependent on Fas/FasL complex in human leukocytes. Hum. Exp. Toxicol. 38, 578–587. doi:10.1177/0960327119828198.
Jiang, Y., Goodwill, J.E., Tobiason, J.E., Reckhow, D.A., 2016. Comparison of the effects of ferrate, ozone, and permanganate pre-oxidation on disinfection byproduct formation from chlorination. In: ACS Symposium Series, pp. 421–437. doi:10.1021/bk-2016-1238.ch016.
Kajjumba, G.W., Attene-Ramos, M., Marti, E.J., 2021. Toxicity of lanthanide coagulants assessed using four in vitro bioassays. Sci. Total Environ. 800, 149556. doi:10.1016/j.scitotenv.2021.149556.
Keucken, A., Heinicke, G., Persson, K.M., Köhler, S.J., 2017. Combined coagulation and ultrafiltration process to counteract increasing NOM in brown surface water. Water (Switzerland) 9, 1–29. doi:10.3390/w9090697.
Komaki, Y., Ibuki, Y., 2022. Inhibition of nucleotide excision repair and damage response signaling by dibromoacetonitrile: A novel genotoxicity mechanism of a water disinfection byproduct. J. Hazard. Mater. 423, 127194. doi:10.1016/j.jhazmat.2021.127194.
Krasner, S.W., McGuire, M.J., Jacangelo, J.G., Patania, N.L., Reagan, K.M., Marco Aieta, E., 1989. Occurrence of disinfection by-products in US drinking water. J. Am. Water Works Assoc. 81, 41–53. doi:10.1002/j.1551-8833.1989.tb03258.x.
Laothong, U., Pinlaor, P., Boonsiri, P., Pairojkul, C., Priprem, A., Johns, N.P., et al., 2013. Melatonin inhibits cholangiocarcinoma and reduces liver injury in Opisthorchis viverrini-infected and N-nitrosodimethylamine-treated hamsters. J. Pineal Res. 55, 257–266. doi:10.1111/jpi.12068.
Li, X.F., Mitch, W.A., 2018. Drinking water disinfection byproducts (DBPs) and human health effects: multidisciplinary challenges and opportunities. Environ. Sci. Technol. 52, 1681–1689. doi:10.1021/acs.est.7b05440.
Liew, D., Linge, K.L., Joll, C.A., 2016. Formation of nitrogenous disinfection by-products in 10 chlorinated and chloraminated drinking water supply systems. Environ. Monit. Assess. 188, 518. doi:10.1007/s10661-016-5529-3.
Lin, E.L.C., Daniel, F.B., Herren-Freund, S.L., Pereira, M.A., 1986. Haloacetonitriles: metabolism, genotoxicity, and tumor-initiating activity. Environ. Health Perspect. 69, 67–71. doi:10.2307/3430372, Vol..
Lipscomb, J.C., El-Demerdash, E., Ahmed, A.E., 2008. Haloacetonitriles: metabolism and toxicity. Rev. Environ. Contam. Toxicol. 198, 169–200. doi:10.1007/978-0-387-09647-6_5.
Lu, G., Qin, D., Wang, Y., Liu, J., Chen, W., 2018. Single and combined effects of selected haloacetonitriles in a human-derived hepatoma line. Ecotoxicol. Environ. Saf. 163, 417–426. doi:10.1016/j.ecoenv.2018.07.104.
Marti, E.J., Pisarenko, A.N., Peller, J.R., Dickenson, E.R.V., 2015. N-nitrosodimethylamine (NDMA) formation from the ozonation of model compounds. Water Res. 72, 262–270. doi:10.1016/j.watres.2014.08.047.
Minister of Health of Canada, 2011. Guidelines for Canadian Drinking Water Quality: Guideline Technical Document N-Nitrosodimethylamine (NDMA). Ottawa, Ontario.
Muellner, M.G., Wagner, E.D., McCalla, K, Richardson, S., 2007. Haloacetonitriles vs. regulated haloacetic acids: are nitrogen-containing DBPs more toxic? Environ. Sci. Technol. 41, 645–651. doi:10.1021/es0617441.
Nicholls, D.G., Budd, S.L., 2000. Mitochondria and neuronal survival. Physiol. Rev. 80, 315–360. doi:10.1152/physrev.2000.80.1.315.
Oliveira, M.M., Teixeira, J.C., Vasconcelos-Nóbrega, C., Felix, L.M., Sardão, V.A., Colaço, A.A., et al., 2013. Mitochondrial and liver oxidative stress alterations induced by N-butyl-N-(4-hydroxybutyl)nitrosamine: relevance for hepatotoxicity. J. Appl. Toxicol. 33, 434–443. doi:10.1002/jat.1763.
Pals, J.A., Ang, J.K., Wagner, E.D., Plewa, M.J., 2011. Biological mechanism for the toxicity of haloacetic acid drinking water disinfection byproducts. Environ. Sci. Technol. 45, 5791–5797. doi:10.1021/es2008159.
Pals, J.A., Wagner, E.D., Plewa, M.J., 2016. Energy of the lowest unoccupied molecular orbital, thiol reactivity, and toxicity of three monobrominated water disinfection byproducts. Environ. Sci. Technol. 50, 3215–3221. doi:10.1021/acs.est.5b05581.
Pals, J., Attene-Ramos, M.S., Xia, M., Wagner, E.D., Plewa, M.J., 2013. Human cell toxicogenomic analysis linking reactive oxygen species to the toxicity of monohaloacetic acid drinking water disinfection byproducts. Environ. Sci. Technol. 47, 12514–12523. doi:10.1021/es403171b.
Parvez, S., Ashby, J.L., Kimura, S.Y., Richardson, S.D., 2019. Exposure characterization of haloacetic acids in humans for exposure and risk assessment applications: An exploratory study. Int. J. Environ. Res. Public Health 16, 471. doi:10.3390/ijerph16030471.
Pegram, R.A., Andersen, M.E., Warren, S.H., Ross, T.M., Claxton, L.D., 1997. Glutathione S-transferase-mediated

mutagenicity of trihalomethanes in Salmonella typhimurium: contrasting results with bromodichloromethane and chloroform. Toxicol. Appl. Pharmacol. 144, 183–188. doi:10.1006/taap.1997.8123.

Pressman, J.G., Richardson, S.D., Speth, T.F., Miltner, R.J., Narotsky, M.G., Hunter, E.S., et al., 2010. Concentration, chlorination, and chemical analysis of drinking water for disinfection byproduct mixtures health effects research: U.S. EPAs four lab study. Environ. Sci. Technol. 44, 7184–7192. doi:10.1021/es9039314.

Richardson, S.D., 2011. Disinfection by-products: formation and occurrence in drinking water. In: Encyclopedia of Environmental Health, ed. J. O. Nriagu, Elsevier BV, Amsterdam, The Netherlands, 2011, pp. 110–136. doi:10.1016/B978-0-444-52272-6.00276-2.

Rider, C.V., Dinse, G.E., Umbach, D.M., Simmons, J.E., Hertzberg, R.C., 2018. Predicting mixture toxicity with models of additivity. In: Rider, C.V., Simmons, J.E. (Eds.), Chemical Mixtures and Combined Chemical and Nonchemical Stressors–Exposure, Toxicity, Analysis, and Risk. Springer International Publishing, Cham, pp. 235–270. doi:10.1007/978-3-319-56234-6_9.

Sakamuru, S., Attene-Ramos, M.S., Xia, M., 2016. Mitochondrial membrane potential assay. Methods Mol. Biol. 1473, 17–22. doi:10.1007/978-1-4939-6346-1_2.

Schlosser, P.M., Bale, A.S., Gibbons, C.F., Wilkins, A., Cooper, G.S., 2015. Human health effects of dichloromethane: key findings and scientific issues. Environ. Health Perspect. 123, 114–119. doi:10.1289/ehp.1308030.

Schwarzenbach, R.P., Gschwend, P.M., Imboden, D.M., 2003. Environmental Organic Chemistry, 2nd ed. John Wiley & Sons. New Jersey doi:10.1002/0471649643.

Sharma, V.K., Yu, X., McDonald, T.J., Jinadatha, C., Dionysiou, D.D., Feng, M., 2019. Elimination of antibiotic resistance genes and control of horizontal transfer risk by UV-based treatment of drinking water: A mini review. Front. Environ. Sci. Eng. 13, 37. doi:10.1007/s11783-019-1122-7.

Stalter, D., O'Malley, E., Von Gunten, U., Escher, B.I., 2016. Fingerprinting the reactive toxicity pathways of 50 drinking water disinfection by-products. Water Res. 91, 19–30. doi:10.1016/j.watres.2015.12.047.

US EPA, 2018. Bioassays for Evaluating Water Quality Screening for total bioactivity to assess water safety. Washington, DC.

US EPA, 2006. Comprehensive Disinfectants and Disinfection Byproducts Rules (Stage 1 and Stage 2): Quick Reference Guide. U. S. Environmental Protection Agency.

Villanueva-Ponce, R., Garcia-Alcaraz, J.L., Cortes-Robles, G., Romero-Gonzalez, J., Jiménez-Macías, E., Blanco-Fernández, J., 2015. Impact of suppliers' green attributes in corporate image and financial profit: case maquiladora industry. Int. J. Adv. Manuf. Technol. 80, 1277–1296. doi:10.1007/s00170-015-7082-6.

Watson, K., Farré, M.J., Knight, N., 2012. Strategies for the removal of halides from drinking water sources, and their applicability in disinfection by-product minimisation: a critical review. J. Environ. Manag. 110, 276–298. doi:10.1016/j.jenvman.2012.05.023.

Weinberg, H.S., Krasner, S.W., Richardson, S.D., Thruston Jr., A.D., 2002. The Occurrence of Disinfection By-Products (DBPs) of Health Concern in Drinking Water: Results of a Nationwide DBP Occurrence Study. U.S. Environmental Protection Agency, Washington.

Yang, C.S., Yoo, J.S.H., Ishizaki, H., Hong, J., 1990. Cytochrome p450IIe1: Roles in nitrosamine metabolism and mechanisms of regulation. Drug Metab. Rev. 22, 147–159. doi:10.3109/03602539009041082.

Zhang, L., Zheng, X.C., Huang, Y.Y., Ge, Y.P., Sun, M., Chen, W.L., et al., 2021. Carbonyl cyanide 3-chlorophenylhydrazone induced the imbalance of mitochondrial homeostasis in the liver of Megalobrama amblycephala: A dynamic study. Comp. Biochem. Physiol.C Toxicol. Pharmacol. 244, 109003. doi:10.1016/j.cbpc.2021.109003.